



ACOUSTICS 2012

An extended geometric model for analysis of string crossings in bowed-string instrument performance

E. Schoonderwaldt^a and M. Demoucron^b

^aInstitute of Music Physiology and Musicians' Medicine (IMMM), Schiffgraben 48, 30175
Hannover, Germany

^bIPEM, Blandijnberg 2, 9000 Gent, Belgium
matthias.demoucron@ugent.be

In earlier motion capture studies of fast repetitive bowing patterns across two and three strings in violin performance it was shown that string crossings were consistently timed earlier than bow reversals. This behavior might have a plausible acoustic explanation: a good attack on the new string requires that bow force is built up before the string can be set in motion. An earlier used feature-extraction model fails to adequately describe the transfer of bow force between strings because it considers string positions and bow inclination transition angles between strings as fixed. An improved model is proposed that (1) takes the compliance of the strings and the bow hair explicitly into account, and (2) includes a correction of string crossing angles for stopped strings. The model requires knowledge of the tensions of the strings and the bow hair, as well as the depth of the fingerboard below the strings. It will be shown how these quantities can be obtained via simple calibrations. The model allows for an accurate calculation of control parameters to drive a virtual violin, allowing to study the relation between bowing movements and the quality of attacks in complex bowing patterns.

1 Introduction

Motion capture of bowing in bowed-string instruments has been employed in a number of recent acoustical and performance studies [1, 2, 3, 4]. This usually involves extraction of bowing parameters and features derived from the tracked position and orientation of the bow and the violin, possibly in combination with sensors, e.g. for measurement of bow force. This information can be used for studying the acoustical function of bowing movements, analyzing bowing techniques, and to drive synthesis models or simulations.

In an earlier approach [5], feature extraction was based on a simplified geometric model of the violin and the bow with fixed string positions. Under certain circumstances, it was found that this model did not reliably detect which string was played, as will be explained in the following section. Furthermore, this model considers the bow inclination range in which the bow is in contact with two adjacent strings as fixed, ignoring the effect of compliance of the strings and the bow. The deficit in adequately describing string transitions was particularly obvious in complex bowing patterns across two adjacent strings, in which one string is stopped and the other is open.

In this paper a refined geometric model of the bow and the violin is proposed that addresses these issues.

2 Improved feature extraction

2.1 Motivation

Figure 1 shows the positions of strings at the bridge, and the fan-shaped areas indicating the ranges in bow inclination associated with playing on the respective strings. In an earlier method for feature extraction, described in Schoonderwaldt and Demoucron [5], these areas were used to determine which string was played, based on bow inclination data obtained from motion capture measurements. It was assumed that the strings were parallel, and that the string positions were fixed (i.e. rigid strings). String crossings (transitions between strings, and double stops) were not adequately described by this model, and a workaround was adopted by introducing arbitrary, fixed inclination areas in which the bow was assumed to be in contact with two adjacent strings. Another deficit of the model was that it did not take into account the displacement of stopped strings. This displacement can lead to considerable deviations of string crossing angles, as much as 5 deg. between adjacent strings when one of them is stopped at half its length (an octave in pitch). As a result, feature extraction was not always accurate, as demonstrated by the example in Fig. 1.

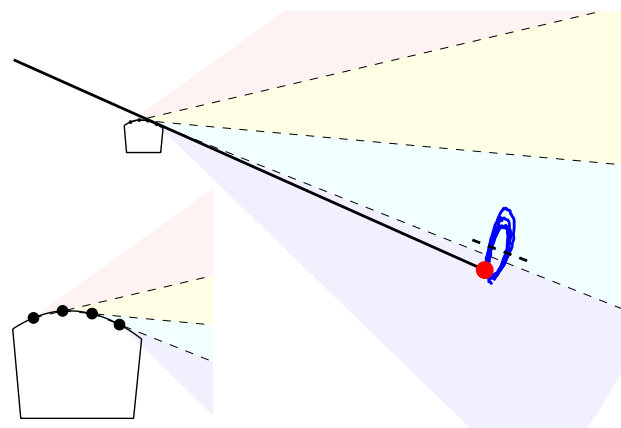


Figure 1: Fixed string positions at the bridge and string crossing angles. The example is a demonstration of that the string crossing angle is not always accurately predicted for stopped strings.

Three major improvements in the proposed model are: 1) the positions of the strings are defined at the bridge *and* at the nut, modeling the strings as non-parallel lines; 2) the depth of the fingerboard below the strings is included, allowing to take into account the displacement of stopped strings; and 3) the compliance of the bow hair and the strings is included in order to model string displacement and bow-hair bending as a function of bow force.

2.2 Fingerboard model

Stopping the string causes a displacement at the bowing point. This can lead to a change in the string crossing angle between adjacent strings when only one of the strings is stopped, or when the strings are stopped at different positions.

The situation is sketched in Fig. 2. The relation between string displacement at the finger position and at the bowing position is

$$h_B = h_S \cdot \frac{y_B}{L_{eff}},$$

where y_B the bow-bridge distance and L_{eff} the effective length of the stopped string.

The fingerboard curve can be estimated by probing h_S at a number of different stop positions. As the fingerboard usually is slightly curved we will describe it by a second order polynomial as a function of relative effective string length ($\lambda = L_{eff}/L_0$):

$$h_S(\lambda) = P_2\lambda^2 + P_1\lambda + P_0. \quad (1)$$

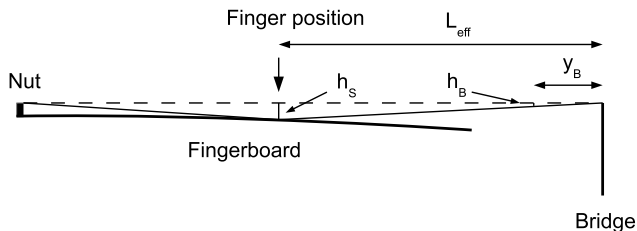


Figure 2: Geometric model of fingerboard (exaggerated proportions).

The change in string crossing angle of a stopped adjacent to an open string is approximately

$$\Delta\theta_c \approx h_B/d,$$

where d the distance between the adjacent strings.

2.3 String transition model

Due to the compliance of the bow hair ribbon and the strings, string transitions are associated with a finite range in inclination. The situation is sketched in Fig. 3, showing a transition from String 1 to String 2. The two panels show the outer limits of the inclination range, demonstrating the contributions of the bending of the string σ_1 and σ_2 (due to yield at the contact point) and the bending of the bow hair γ to the total transition range

$$\delta = \gamma + \sigma_1 + \sigma_2. \quad (2)$$

The bending of the bow hair under influence of loading (with force F_n) can be calculated via a graphical construction shown in Fig. 4. In a small angle approximation, the relation

$$F_n = T_{bh} (\sin \alpha_1 + \sin \alpha_2) \approx T_{bh} (\alpha_1 + \alpha_2)$$

allows us to express γ in terms of bow force F_n and bow hair tension T_{bh} :

$$\gamma = \alpha_1 + \alpha_2 \approx \frac{F_n}{T_{bh}}. \quad (3)$$

The yield of the strings at the bow-string contact point (x in Fig. 4) can be derived via a similar construction:

$$\Delta s_i \approx \frac{F_n}{T_i} L_i (\beta_i - \beta_i^2),$$

where i the string index, T_i the string tension, L_i the effective length of the string, and β_i the bow-bridge distance normalized with respect to the effective string length L_i . Given the

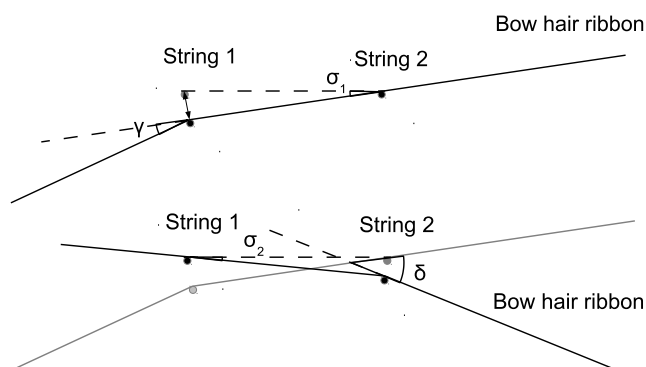


Figure 3: Geometric string transition model (exaggerated proportions).

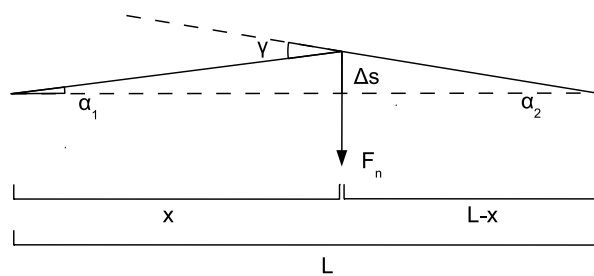


Figure 4: Transverse displacement of the loaded bow-hair ribbon (or string).

distance d_{ij} between adjacent strings, the angle σ_i in Fig. 3 can be expressed in terms of bow force and string tension:

$$\sigma_i \approx \frac{\Delta s_i}{d_{ij}} = \frac{F_n}{T_i} \cdot \frac{L_i (\beta_i - \beta_i^2)}{d_{ij}}. \quad (4)$$

Inserting (3) and (4) in (2) now gives us the string transition range as a function of measurable quantities:

$$\delta = F_n \left[\frac{1}{T_{bh}} + \frac{1}{d_{ij}} \left(\frac{L_i (\beta_i - \beta_i^2)}{T_i} + \frac{L_j (\beta_j - \beta_j^2)}{T_j} \right) \right]. \quad (5)$$

It should be noted that the inter-string-distance d_{ij} also depends on bow-bridge distance for non-parallel strings. Furthermore, L_i and β_i depend on the pitch played (stop position).

When the bow is in contact with two adjacent strings, e.g. during string transitions or double stops, the total bow force is proportionally distributed amongst the strings with respect to inclination.

2.4 Practical implementation

An important additional requirement was that the model should be suitable for practical implementation, based on quantities that are reliably measurable with available techniques, and without the need for overly elaborate calibration procedures.

Fingerboard probing. The depth of the fingerboard below the strings was determined using a digitizing probe, a pen with four reflective markers, the position of which was tracked with the motion capture system. A baseline was constructed by probing the string at the bridge and at the nut, then the string was pushed down to the fingerboard with the probe at several (at least six) stop positions, yielding a series of displacements h_s (see Fig. 2). Then, for each string a polynomial fit of string displacement as a function of stop position was obtained via Eq. (1). The coefficients P_{2-0} allow to estimate the string depth at any stop position. This procedure needs only be performed once per individual instrument.

Tuning calibration. In the earlier method a so-called *tuning* calibration was performed, in which the string-crossing inclinations were determined by softly playing the double string combinations. The positions of the strings at the bridge could then be calculated by geometric calculations given the distances between adjacent strings. In the improved model,

a similar procedure is used, however, the tuning trial is extended by playing the double string combinations close to the nut, as well. The positions of the strings at the bridge and at the nut can then be calculated given the distances between adjacent strings at the bridge and at the nut (e.g. measured using a caliper).

Tension calibration. The tension of the bow hair can be determined from the bow-force calibrations, that are already routinely performed for calibration of the bow force sensor (see [6] and [5]). During this calibration the bow is pressed against a stiff load cell (force transducer) at several positions along the bow. The geometric model of the bow (see [5]) is used for estimation of the transverse displacement of the bow hair. The bow hair tension is then obtained via inverse calculation of Eq. (3).

For the string tensions we rely on specifications of the manufacturer (Pirastro).

It should be noted that the fingerboard probing and the bow hair tension calibration can only be reliably performed using high-quality motion capture data at sub-millimeter resolution.

3 Model evaluation

Measurements were performed using a Qualisys motion capture system with seven Oqus 3+ cameras in a circular configuration at a distance of 2-3 m from the tracked objects. Bow force was measured with a bow force sensor [6]. The inclination of the bow was calculated relative to the violin. For a detailed description of the method for tracking the position and orientation of the violin and the bow and the extraction of bowing parameters, see Schoonderwaldt and Demoucron [5].

The proposed model was evaluated by comparing the predicted values of string crossing angle and string transition width with inclination measured in playing tasks, that were specially designed to single out these features.

The numerical implementation (in Matlab) of the proposed model provided instantaneous values of the string crossing angle θ_c and the string transition range δ as a function of measured values of bow force and bow-bridge distance. The stop positions were added manually, based on knowledge of the played pitch.

3.1 String crossing angle

The dependance of string crossing angle on stop position was empirically determined by lightly and slowly playing double stops, performing a series of pitches on one string (in cent: 0 (open), 200, 500, 900, 1200 (half length), and 1700), while the other string was open. The difference between measured (average) inclination and predicted string crossing angles is shown in Fig. 5. The top panel clearly shows the deficit of a fixed string crossing angle: the predicted value was only correct when both strings were open, and there is a clear increase in error with increasing stop position (i.e. decreasing L_{eff}/L_0 value), up to almost 6 deg. at high positions. The proposed model performed much better: the error remained within 0.5 deg. at the whole range. Similar results were found for other stopped-open string combinations.

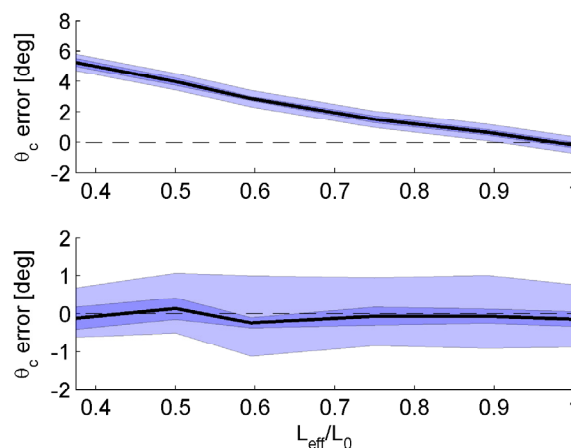


Figure 5: Evaluation of predicted string crossing angle as a function of stop position: (top) for a fixed transition angle (earlier model), and (bottom) based on the proposed fingerboard model. The black lines indicate the difference between inclination measured during performance and predicted string-crossing angles, the dark-shaded areas indicate the standard deviation of measured inclination, and the light-shaded areas indicate the estimated string transition range (fixed value top panel).

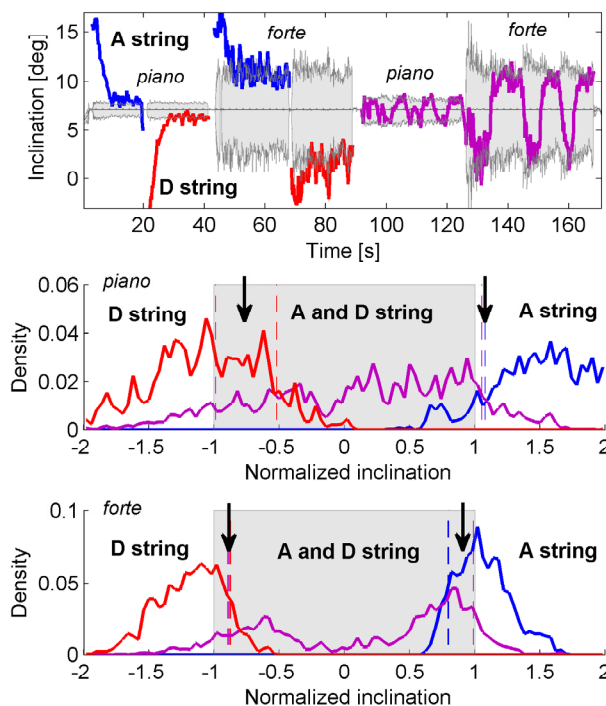


Figure 6: (Top) Inclination transition range predicted by the model (shaded area) and inclination during playing (colored lines: blue = A string, red = D string, purple = double-string playing). (Middle, bottom) Density curves of inclination during playing, normalized with respect to the predicted inclination range (shaded area); separate density curves for (middle) piano and (bottom) forte. The dashed lines show the 10th and the 90th percentiles of the distributions, which were used for estimation of empirical transition range limits.

3.2 String transition range

The string transition range was empirically determined by playing open strings in two complementary tasks: (a) playing single strings, trying to play as close as possible to the adjacent string (incidentally touching); (b) playing double strings, trying to find the inclination limits at which the strings are still both in contact with the bow (incidentally losing contact). Both tasks were performed piano and forte, as well as far from bridge and close to bridge.

Figure 6 shows that there was a good agreement between measured inclination and the predicted limits of the string transition range. The two lower panels show the inclination distribution curves corresponding to the playing tasks, normalized with respect to the transition range (between -1 and 1). The empirical values of the transition limits were estimated by taking the averages of the 10th and 90th percentiles of the overlapping distributions, e.g. the average of the 90th percentile of the double stop distribution and the 10th percentile of the A string distribution (right arrow). The empirically found limits were generally close to -1 and 1 in all conditions (piano/forte, close to/far from the bridge), indicating a good agreement. There was a tendency that the empirically determined ranges were slightly smaller than the model predictions. The reason for this is unclear, but it could be due to the test procedure.

3.3 Playing test

As a final playing test, a passage was recorded of fast détaché notes played on alternating strings, forming circular bowing patterns as shown in Fig. 1. Fig. 7 shows examples of forte and piano performances. The top panel clearly demonstrates that the string transition range can be highly variable during performance. The lower panel shows the bow force exerted on individual strings, a new feature that can be extracted using the proposed model, that will be useful for further acoustical studies of note transitions in complex bowing patterns.

4 Discussion and conclusion

A refined model was presented for accurate description of string crossings and string transitions from motion capture measurements, suitable for analysis of complex bowing patterns and double-stops playing. The model includes calculation of the string crossing angle as a function of stop position, as well as the string transition range taking into account the compliance of the bow hair and the strings.

Interestingly, the angular ranges in which two neighboring strings are in contact with the bow can be as much as 10 deg., which is comparable to the angular range for playing individual strings. Furthermore, it was shown that string crossing angles and string transition width is highly variable, implying that the performer has to respond to constantly changing performance constraints.

An important result is that the model can provide force signals of individual strings, making it possible for the first time to perform detailed acoustical studies on the physical conditions for good note transitions in complex bowing patterns, for example by means of simulation [1, 7].

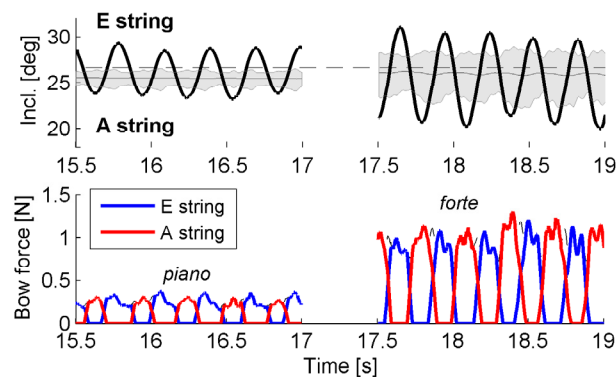


Figure 7: Playing test: circular bowing patterns across two strings, played piano (left) and forte (right).

Acknowledgments

Erwin Schoonderwaldt receives a two-year postdoctoral fellowship by the Alexander von Humboldt Foundation, Germany.

References

- [1] M. Demoucron, *On the control of virtual violins: Physical modelling and control of bowed string instruments*. PhD thesis, Université Pierre et Marie Curie (UPMC), Paris & Royal Institute of Technology (KTH), Stockholm (2008)
- [2] E. Schoonderwaldt, *Mechanics and acoustics of violin bowing: Freedom, constraints and control in performance*. PhD thesis, KTH – School of Computer Science and Communication, Stockholm, Sweden (2009)
- [3] A. Perez, *Enhancing Spectral Synthesis Techniques with Performance Gestures using the Violin as a Case Study*. PhD thesis, Universitat Pompeu Fabra, Barcelona, Spain (2009)
- [4] E. Maestre, *Modeling Instrumental Gestures: An Analysis/Synthesis Framework for Violin Bowing*. PhD thesis, University Pompeu Fabre, Barcelona, Spain (2009)
- [5] E. Schoonderwaldt and M. Demoucron, “Extraction of bowing parameters from violin performance combining motion capture and sensors,” *J. Acoust. Soc. Am.*, vol. 126, no. 5, pp. 2695–2708 (2009)
- [6] M. Demoucron, A. Askenfelt, and R. Caussé, “Measuring bow force in bowed string performance: Theory and implementation of a bow force sensor,” *Acta Acustica united with Acustica*, vol. 95, no. 4, pp. 718–732 (2009)
- [7] K. Guettler, “On the creation of the Helmholtz motion in bowed strings,” *Acta Acustica united with Acustica*, vol. 88, no. 6, pp. 970–985 (2002)